Rheol Acta (2013) 52:801–814
DOI 10.1007/s00397-013-0706-6

ORIGINAL CONTRIBUTION

Viscoelastic melt rheology and time–temperature superposition of polycarbonate–multi-walled carbon nanotube nanocomposites

Gabriel Y. H. Choong · Davide S. A. De Focatiis · David G. Hassell

Received: 3 May 2012 / Revised: 8 February 2013 / Accepted: 8 April 2013 / Published online: 26 May 2013

Abstract This work investigates the linear and non-linear viscoelastic melt rheology of four grades of polycarbonate melt compounded with 3 wt% Nanocyl NC7000 multi-walled carbon nanotubes and of the matching matrix polymers. Amplitude sweeps reveal an earlier onset of non-linearity and a strain overshoot in the nanocomposites. Mastercurves are constructed from isothermal frequency sweeps using vertical and horizontal shifting. Although all nanocomposites exhibit a second plateau at $\sim 10^5$ Pa, the relaxation times estimated from the peak in loss tangent are not statistically different from those of pure melts estimated from cross-over frequencies: all relaxation timescales scale with molar mass in the same way, evidence that the relaxation of the polymer network is the dominant mechanism in both filled and unfilled materials. Non-linear rheology is also measured in large amplitude oscillatory shear. A comparison of the responses from frequency and amplitude sweep experiments reveals the importance of strain and temperature history on the response of such nanocomposites.

G. Y. H. Choong · D. S. A. De Focatiis (✉)
Division of Materials, Mechanics and Structures,
University of Nottingham, Nottingham NG7 2RD, UK
e-mail: davide.defocatiis@nottingham.ac.uk

G. Y. H. Choong
e-mail: ezzgc@nottingham.ac.uk

D. G. Hassell
Department of Chemical and Environmental Engineering,
University of Nottingham Malaysia Campus,
Semenyih, Selangor 43500, Malaysia
e-mail: david.hassell@itb.edu.bn

D. G. Hassell
Petroleum and Chemical Engineering,
Institut Teknologi Brunei, Gadong BE 1410,
Brunei Darussalam

Keywords Polycarbonate · Multi-walled carbon nanotubes · Melt rheology · Linear viscoelasticity · Non-linear viscoelasticity · Time–temperature superposition

Introduction

The addition of multi-walled carbon nanotubes (MWCNT) to polymeric matrices has stimulated significant interest within the research and industrial communities. The attraction of such nanocomposites arises because of the potential to benefit from the outstanding properties of MWCNTs whilst retaining the ease of processing of polymeric matrices. By doing so, it has been possible to generate new families of materials that are melt-processable with standard equipment but that outperform commodity plastics in terms of material properties. These properties include higher mechanical strength (Cadek et al. 2002; Eitan et al. 2006; Fornes et al. 2006) and substantially higher electrical conductivities (Curran et al. 2009). The benefit of employing MWCNTs over conventional fillers in thermoplastics is that they have very high aspect ratios, enabling the nanocomposites to exhibit noticeable property improvements even at relatively low filler content. This is essential for retaining the desirable processing attributes of the polymeric matrix.

At present, polycarbonate (PC) nanocomposites are used in electronic static discharge protection applications. The material's increased abrasion resistance, and consequently low shedding of particles, minimises contamination, making it an ideal candidate for components in clean room manufacturing, such as trays for the handling of integrated circuits and semiconductors. The electrical conductivity imparted on the nanocomposites by the MWCNTs allows the build-up of static charges that can damage the delicate electronic

components to be safely dissipated. This is achieved by enabling the flow of electrical charge through a percolating network of nanotubes embedded in the polymer matrix. Such a network is formed by appropriate dispersion of the MWCNTs in the matrix during processing.

There are a multitude of factors that influence the performance of a nanocomposite, but filler dispersion is generally acknowledged to be among the most significant. One of the most interesting aspects of dispersion is the role it plays in optimising different properties—for instance, optimal mechanical performance is generally associated with homogeneous and uniform filler dispersion, whereas high degrees of electrical conductivity arise through an appropriate degree of clustering and network formation (Alig et al. 2012).

Other important factors identified as playing a role in the performance of nanocomposite products can be split into carbon nanotube (CNT)-related factors and polymer processing-related factors. CNT factors include surface defects (Yamamoto et al. 2010), surface modification (Spitalsky et al. 2010), waviness (Fisher et al. 2002), and orientation (Pötschke et al. 2005; Dijkstra et al. 2010). Processing-related factors include the rheology of the polymer matrix (Cadek et al. 2002) and the interrelated compounding process conditions (Lew et al. 2009, 2011). The large number of variables renders direct comparison of different studies challenging.

Several authors have specifically studied the properties of PC–MWCNT composites, focusing on the melt rheology (Pötschke et al. 2002; Du et al. 2004; Abdel-Goad and Pötschke 2005; Sung et al. 2005; Alig et al. 2008), the mechanical response (Eitan et al. 2006; Fornes et al. 2006; Satapathy et al. 2007), and the electrical properties (Du et al. 2004; Sung et al. 2006; Alig et al. 2008; Saphiannikova et al. 2012). Some authors have employed a combination of characterisation methods, such as the simultaneous electrical and rheological measurements of Alig et al. (2008) and Zeiler et al. (2010). These authors observed a reversible formation of the filler network, evident from the time-dependent recovery of both electrical and mechanical properties after applying shear deformation to PC–MWCNT melts. They employed percolation theory and agglomeration kinetics to explain their observations and attributed the changes in electrical conductivity and storage modulus to the destruction and reformation of CNT agglomerates. Alig and co-workers (2008), thus, concluded that the process of agglomeration of CNTs plays a crucial role in determining both of these physical properties of the nanocomposite. Zeiler et al. (2010) used a similar investigation method to study the influence of polymer viscosity and of polymer–nanotube interactions on network formation by exploring both the linear and the non-linear viscoelastic regions. They observed that the formation of both rheological and electrical networks was faster at higher temperatures, as well as in nanocomposites with a matrix of lower molar mass and, hence, lower viscosity. They measured a higher storage modulus in nanocomposites with matrices of lower molar mass and suggested that the shorter polymer chains facilitated CNT–CNT contacts, giving rise to a stiffer nanotube network. They concluded that the breakup of CNT clusters and the diffusion-controlled clustering of CNTs are two opposite processes which superpose, and that the timescale of the diffusion-controlled clustering is not influenced by oscillatory shear flow. Thus, it is apparent that the polymer matrix can have a strong influence on the rheological properties following breakup of CNT clusters. In order to reconcile their observations, Zeiler and co-workers (2010) proposed an extension to the models of Alig et al. (2008) and Pötschke et al. (2004) in which the CNT network consists of weakly bonded clusters that breakup and reaggregate. More recently, Handge et al. (2011) applied a fractional Zener model for predictions of linear viscoelastic properties of PC–MWCNT melts to the experimental data of Zeiler et al. (2010), and they were successful in describing the storage modulus over a wide frequency range, but less so for the loss modulus.

Time–temperature superposition (TTS) is a methodology integral to most modelling efforts that combines the effects of time and temperature and that relies on the principle of thermorheological simplicity. Materials are considered thermorheologically simple when all relaxation mechanisms present have the same temperature dependence (Dealy and Plazek 2009). In polymer melts, the temperature dependence of relaxation times allows frequency-dependent or time-dependent viscoelastic data to be shifted to any reference temperature through an appropriate shift factor. This process is normally referred to as *horizontal* shifting. The viscoelastic modulus of polymer melts is also weakly dependent on temperature because of its effect on density. When a temperature correction is applied to the modulus, it is known as *vertical* shifting (Rubinstein and Colby 2003).

There have been mixed conclusions on the application of TTS to nanocomposites. Handge and Pötschke (2007) attempted to shift the frequency dependence of viscoelastic moduli of PC–MWCNTs (2 wt%) measured at 190 and 210 °C and observed that the data superposed unsatisfactorily. They suggested that the failure of TTS implied that the relaxation processes of the pure polymer and of the filler network had different temperature dependence, and they attributed the influence of interactions between the polymer and filler more to the entropy elasticity of the melt than to the temperature. Solomon et al. (2001)

successfully applied TTS to melt-compounded polypropylene filled with organophilic nanoclay in the presence of a compatibilizer. They observed a similar temperature dependence of shift factors in the nanocomposites as in the base polymer. Reichert et al. (2001) found that the application of TTS was possible with extruded and injection-moulded polypropylene filled with organophilic layered silicates that were annealed, but, interestingly, that TTS was not possible without the annealing step. They used the shifting procedure as a tool for the investigation of clay platelet network formation and observed that the annealing process improves exfoliation and facilitates the formation of a thermodynamically stable structure. Wu et al. (2007) observed that TTS was possible in poly(butylene terephthalate)–MWCNT nanocomposites in a narrow temperature window of 230 to 240 °C, but not at higher temperatures up to 260 °C. They attributed the successful superposition at higher reduced frequencies to dominant local chain dynamics and the failure of superposition at lower reduced frequencies to the different temperature dependence of the percolated network. None of the reported studies attempted any application of vertical shifting.

This work investigates the linear and non-linear viscoelastic melt rheology of a range of PC–MWCNT nanocomposites of constant filler content but varying matrix viscosity and of the matching pure melts. The aim is to elucidate the roles played by nanotubes and by the matrix polymer on several aspects of the viscoelastic response: time–temperature superposition and vertical shifting, dynamic strain amplitude, relaxation processes, and strain and temperature history.

Experimental

Materials

Four grades of PC ranging from low viscosity to high viscosity were supplied as granules by Bayer Material Science AG. Nanocyl NC7000 MWCNTs were manufactured by Nanocyl S.A., Belgium, via a catalytic chemical vapour deposition process. Castillo and co-workers (2011) reported measurements of the average diameter and length of Nanocyl NC7000 nanotubes prior to processing as 10 and 1,341 nm, respectively. The molar mass of each of the supplied PC grades was measured in tetrahydrofuran relative to polystyrene standards using an Agilent Technologies PC-GPC 120, and measurements of the number-average and weight-average molar masses are reported in Table 1.

Table 1 Measurements of molar mass obtained via GPC for the PC materials used in this study

Materials	M_n (g mol^{-1})	M_w (g mol^{-1})	Polydispersity index (PDI)
Makrolon PC 2205	13,900	33,600	2.46
Makrolon PC 2405	14,200	38,700	2.73
Makrolon PC 2805	18,000	45,700	2.59
Makrolon PC 3105	21,400	50,500	2.40

Nanocomposite preparation

Nanocomposites were melt compounded by Nanocyl using an Industrial Leistritz ZSK-MAXX co-rotating twin screw extruder with a screw length to diameter ratio of 48:1. The MWCNTs were gravimetrically fed into each PC melt through a side feeder, with the nanotubes making up a mass fraction of 3.0 wt% (volume fraction of 2.1 %)[1] for all PC grades. The screw speed was fixed at 300 rpm, and the barrel temperature was fixed at 280 °C for all materials. The extrudate was pelletised into granules for later moulding. Soxhlet extraction of PC resin from the nanocomposite after processing demonstrated that no degradation of the polymer matrix took place during compounding.

Thermal characterisation

Differential scanning calorimetry (DSC) measurements were performed with a TA Instruments DSC Q10 at a scan rate of 10 °C min^{-1} from 25 to 250 °C in a nitrogen atmosphere on both filled and unfilled PC. The glass transition temperatures, T_g, were identified as the average temperatures of the peaks of the derivatives of heat flow with respect to temperature from three separate measurements during the second heating cycle. Values reported in Table 2 are averages and standard errors obtained from three independent measurements on each material.

Thermogravimetric analysis of PC and PC–MWCNTs was performed with a SDT Q600 TA under both air and nitrogen atmospheres. The onset of degradation, defined by 5 % of weight loss, was observed to occur above 440 °C for all the materials in both atmospheres.

Rheological measurements

Circular discs of 30 mm in diameter and 0.5 mm in thickness were compression moulded using an in-house heated

[1]Calculated using ρ_{PC} =1.19 g cm^{-3} from Bayer MaterialScience (2009) datasheet and ρ_{CNT} = 1.75 g cm^{-3} (Shaffer and Windle 1999).

Table 2 Glass transition temperatures determined by DSC of all materials

Materials	T_g(°C)
Unfilled	
Makrolon PC 2205	146.0 ± 0.2
Makrolon PC 2405	147.4 ± 0.2
Makrolon PC 2805	146.5 ± 0.4
Makrolon PC 3105	147.6 ± 0.4
MWCNT-filled (3 wt%)	
Makrolon PC 2205	146.0 ± 0.5
Makrolon PC 2405	146.5 ± 0.2
Makrolon PC 2805	145.2 ± 0.7
Makrolon PC 3105	147.0 ± 0.8

press. Prior to moulding, granules of PC and nanocomposite were dried in an air-circulating oven at 80 °C for a minimum of 8 h. Moulding was carried out at 250 °C, including a 10 min warm-up period, a 5 min stage in which the pressure was applied and released repeatedly in order to dislodge trapped air, and a further 5 min at the moulding temperature under light pressure to allow for consistent relaxation of the polymer. After this time, cold water was flushed through channels in the heated platens, cooling the mould at a repeatable rate of ∼10–15 °C min^{-1}. The mould was removed from the press once the temperature was sufficiently below T_g of the polymer.

Dynamic rheometry was performed using a Bohlin C-VOR Instruments rheometer fitted with environmental chamber. Measurements were performed in stress-controlled oscillatory shear using a 25 mm parallel plate geometry with a 0.5 mm gap size in an air atmosphere. Each moulded disc was allowed to acclimatise at the highest temperature of testing for a period of 5 min and trimmed to size with a sharp blade prior to commencing the test. The auto-tension option was enabled during the tests to compensate for thermal expansion of the specimen. A thermal equilibration time of 5 min followed by a 30 s buffer delay was imposed before beginning each isothermal test run.

Isothermal amplitude sweeps at logarithmically increasing shear strains between 0.01 and 100 % were performed at a fixed frequency of 2π rad s^{-1} on pure and MWCNT-filled PC 2205. Isothermal frequency sweeps were carried out in decreasing 20 °C steps between 260 and 160 °C for all grades of pure PC and between 300 and 160 °C for all nanocomposite grades, at logarithmically increasing frequencies from 0.2 to 80π rad s^{-1}, at a fixed strain amplitude of 0.5 %. Isothermal frequency sweeps were also performed at strain amplitudes of 0.05, 5 and 50 % for MWCNT-filled PC 2205 only. Limited experiments were performed in increasing 20 °C steps, although no significant differences were observed in the measured data as a result of the change of direction of the temperature step.

Results and discussion

Amplitude sweeps

Figure 1 reports the storage modulus G' and the loss modulus G'', both normalised with respect to their measured values at 0.5 % strain $G'_{0.5\,\%}$ and $G''_{0.5\,\%}$, respectively, for both unfilled and filled PC 2205, as a function of strain amplitude measured at 2π rad s^{-1} for all temperatures investigated. The normalisation is intended to facilitate the determination of a strain amplitude for which both filled and unfilled PC are within the linear viscoelastic (LVE) region.

Very small strain amplitudes, <0.1 %, result in noisier measured signals, as the torques and angular velocities approached the limits of the resolution of the instrument. A region where moduli are independent of strain amplitude then appears with increasing amplitude, extending to strains beyond 10 % strain for the unfilled PC, but only to 0.5 % strain for the filled PC. The earlier onset of non-linearity has been previously attributed to the effect of strain amplification: the matrix experiences a higher local strain than the macroscopic strain due to the presence of the stiff nanotubes (Richter et al. 2009; Costa et al. 2008). This effect is generally enhanced by confinement of polymer chains located near the surface of a nanotube (Stöckelhuber et al. 2011; Vilgis 2005). Since no specific surface modification of MWCNTs was performed in our materials, chemical interactions between the matrix and CNTs are likely to be weak. Nevertheless, the confined or adsorbed layer should be detectable by its reduction to the mobility of chains, leading to a rise in T_g. Measurements obtained from DSC reported in Table 2 indicate a small but discernible *reduction* in T_g with the addition of MWCNTs. Although the presence of MWCNTs causes an increase in T_g for most polymers, Castillo and co-workers (2011) also observed a reduction in T_g in a wide range of PC nanocomposites similar to those of this study and attributed its presence either to matrix degradation (not present in this study) or to particularly favourable interactions between PC and MWCNTs leading to a reduction in the degree of entanglement of chains near the CNT surfaces.

At larger strain amplitudes, the most striking difference in the response arising from the presence of filler is a strain overshoot in loss modulus. This overshoot reaches a maximum at shear strains of 5–10 % and is followed by shear thinning behaviour at even larger strains. Similar overshoots were previously observed in polyamide-6 clay nanocomposites (Wan et al. 2005) and have been attributed to and can be modelled by the different amplitude dependence of the rate

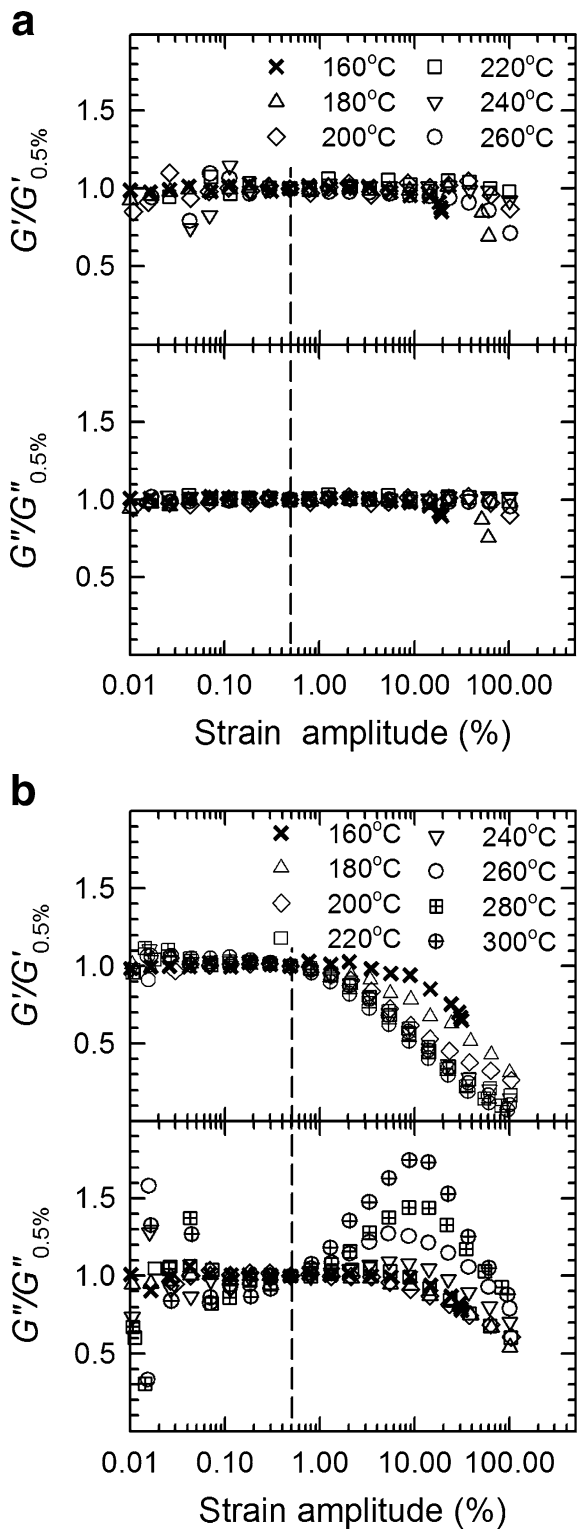

Fig. 1 Amplitude sweeps of normalised storage modulus $G'/G'_{0.5\,\%}$ and loss modulus $G''/G''_{0.5\,\%}$ measured at 2π rad s^{-1} of (**a**) unfilled PC 2205 at temperatures 160–260 °C and of (**b**) PC–MWCNT (3 wt%) 2205 at temperatures 160–300 °C. The vertical *dashed line* indicates the linear viscoelastic limit

of cluster formation relative to that of cluster destruction (Hyun et al. 2011). A cluster in this context can be thought of as a region of material in which there is increased CNT connectivity. The overshoot is greater at higher temperatures. This is consistent with the rate of cluster formation being a temperature-dependent process. The destruction of CNT clusters with increasing strain amplitude also provides an explanation for the earlier onset of non-linearity in storage modulus in the filled materials.

In subsequent experiments, linear viscoelasticity was explored through isothermal frequency sweeps performed at a strain amplitude of 0.5 %, indicated in Fig. 1, where both filled and unfilled PC is within the LVE at all temperatures of interest. It is noted that while the LVE limit was explored using a fixed frequency of 2π rad s^{-1}, the applicability across a wide temperature range suggests that it will be equally appropriate across a wide frequency range.

Construction of mastercurves

Vertical shifting

Dealy and Plazek (2009) recommended the use of the van Gurp–Palmen (VGP) plot of loss angle δ vs. complex modulus G^* to ascertain the thermorheological simplicity of a material. The VGP plot does not require a shift in frequency to a reference temperature to produce overlapping curves but only a shift in modulus with temperature (van Gurp and Palmen 1998). Figure 2a illustrates unshifted isothermal frequency sweeps at 0.5 % strain for both filled and unfilled PC 2205 as a VGP plot.

The measurements on unfilled PC exhibit a reasonably good but not perfect overlap across the temperature range; the measurements on PC–MWCNT show a distinct lack of overlap. A common method of accounting for changes in modulus with temperature T in pure polymer melts is to apply a density ρ correction to the modulus such that the relationship

$$\frac{G^*(T_{\mathrm{ref}})}{\rho_{\mathrm{ref}} T_{\mathrm{ref}}} = \frac{G^*(T)}{\rho T} \tag{1}$$

is satisfied, where T_{ref} is the reference temperature and ρ_{ref} is the density at this reference temperature. The ratio $\rho_{\mathrm{ref}} T_{\mathrm{ref}}/\rho T = b_{\mathrm{T}}$ is the *vertical* shift factor (noting that, in practice, it results in a horizontal shift in a VGP plot). A convenient expression for the density of PC ρ_{PC} was obtained by Zoller (1982) from isothermal dilatometry experiments as

$$\rho_{\mathrm{PC}} = \exp\left[0.307 - 1.859 \times 10^{-5}(T + 273)^{3/2}\right]. \tag{2}$$

Variations in density with molar mass are small and neglected here. The computed value of b_{T} is shown in Fig. 3.

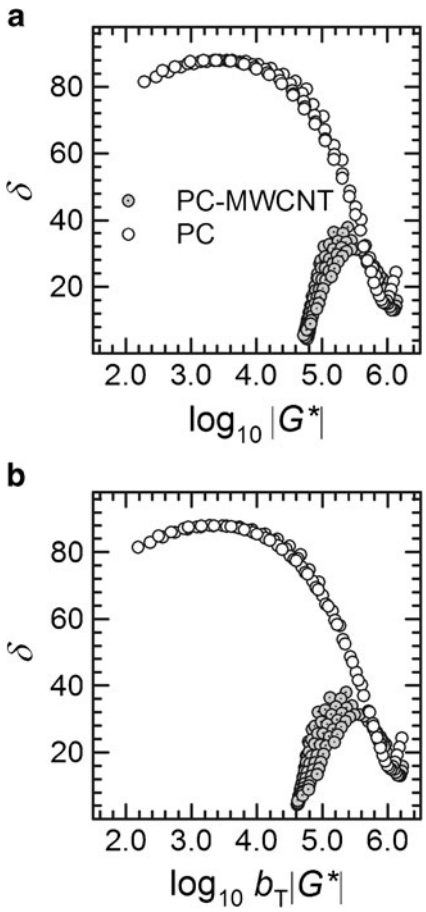

Fig. 2 **a** Van Gurp–Palmen plot of phase angle vs. complex modulus over a temperature range of 160–260 °C for unfilled PC 2205 and of 160–300 °C for PC–MWCNT 2205 (3 wt%). **b** Same plot vs. reduced complex modulus at $T_{ref} = 200$ °C

Using Eqs. 1 and 2, a reduced modulus ($b_T G^*$) VGP plot for unfilled PC 2205 at $T_{ref} = 200$ °C is produced and shown in Fig. 2b. An improvement to the overlap between temperatures can be observed relative to the unshifted data in Fig. 2a.

A similar approach was attempted with the nanocomposite. To the authors' knowledge, there are no reports in the literature on variation in density with temperature of MWCNTs. Hence, a constant density of $\rho_{CNT} = 1.75$ g cm^{-3} (Shaffer and Windle 1999) was used across the temperature range. The density of filled PC was determined from the mass fraction of nanotubes x as

$$\rho = \frac{\rho_{PC}\rho_{CNT}}{x\rho_{PC} + (1-x)\rho_{CNT}}. \quad (3)$$

The computed value of b_T based on density is also shown in Fig. 3 for the PC–MWCNTs. It is virtually indistinguishable from that of the pure PC due to the small fraction of CNTs in these nanocomposites.

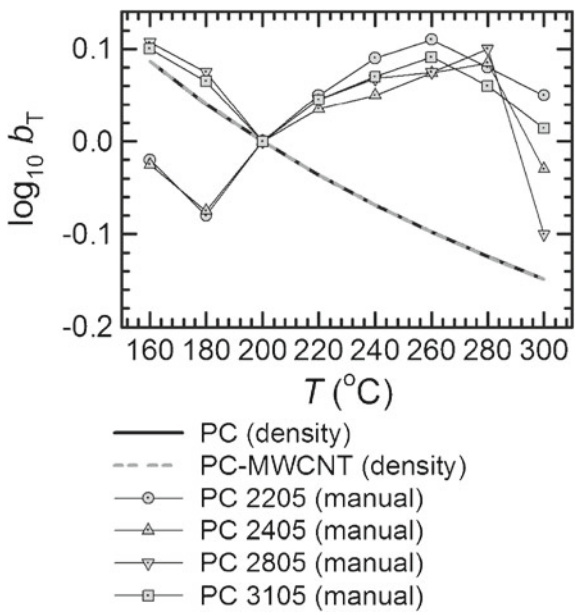

Fig. 3 Vertical shift factors at reference temperature $T_{ref} = 200$ °C determined for unfilled PC based on a density correction using Eqs. 1 and 2 (*thick solid line*), and for PC–MWCNT using Eqs. 1 and 3 (*thick dashed line*). Vertical shift factors obtained by manual shifting using the VGP plots for filled PC grades (*symbols*). The *thin lines* are a guide to the eye

A reduced modulus VGP plot for the filled PC 2205 at a reference temperature of 200 °C using the density correction is shown in Fig. 2b. The correction is actually detrimental to the quality of the superposition, suggesting that there may be a different reason for the change in modulus with temperature in the filled systems. As a step towards understanding this process, the vertical or modulus shift factors, b_T, are obtained by determining the (horizontal) shift in complex modulus required to superpose the measurements in the VGP plot.

b_T was obtained manually, from a visual assessment of the overlap for measurements on all filled grades, and is shown in Fig. 3. Although it is possible to achieve overlap in the low-frequency region of the measurements, it is challenging to achieve overlap in the high-frequency range in all temperatures except for 160 °C. One example of a manually shifted VGP plot is shown in Fig. 4 for filled PC 2205. There are no significant differences in either b_T or the quality of fit between matrix grades at temperatures above 200 °C; at temperatures below 200 °C, there appears to be some effect of molar mass, although the reason for this is unclear.

Horizontal shifting

A numerical procedure was employed to determine the optimal amount of horizontal shift in the frequency domain of

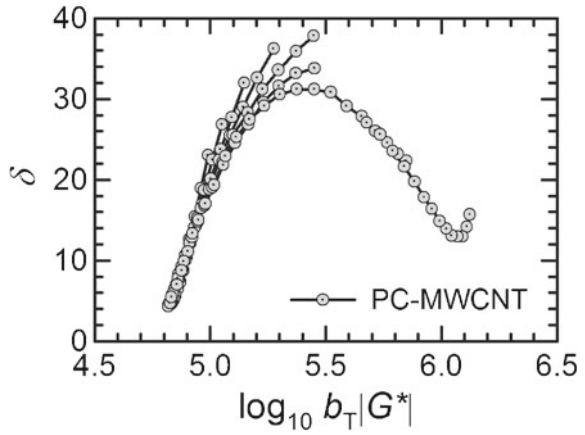

Fig. 4 Shifted van Gurp–Palmen plot for PC–MWCNT 2205 (3 wt%) at a reference temperature of $T_{ref} = 200$ °C used to determine the vertical shift factor. The *lines* are a guide to the eye

the reduced moduli required to attempt the production of a mastercurve. For every measurement temperature T, a horizontal shift factor a_T was identified relative to a fixed reference temperature T_{ref} that minimises the error in the overlap of the shifted moduli measurements relative to the adjacent measured temperature. The method is based on that suggested by Gergesova et al. (2010), and full details are provided in the Appendix. Horizontal shift factors obtained using this procedure are shown in Fig. 5a for unfilled grades and in Fig. 5b for filled grades.

Horizontal shift factors are relatively independent of both matrix polymer and of the presence of nanotubes. For sufficiently entangled unfilled polymer melts, this is expected. The similarity of shift factors between the filled and pure materials is evidence that the relaxation processes probed in this temperature range all have the same temperature dependence (even though the moduli do not).

Mastercurves

The shift factors shown in Figs. 3 and 5a are used to produce reduced frequency–modulus mastercurves for the different grades of unfilled PC used in this study. These are illustrated in Fig. 6. As is well known in the literature on polymer melts, the width of the rubbery plateau increases with increasing molar mass and flow occurs at a lower reduced frequency. In unfilled PC, at low reduced frequencies, loss modulus is always higher than the storage modulus (as can be seen for PC 2205 in the inset of Fig. 6), and the materials exhibit liquid-like properties typical of polymer melts with the characteristic gradients in the terminal zone of $G' \propto \omega^2$ and $G'' \propto \omega$.

The shift factors shown in Figs. 3 and 5b are used to produce reduced frequency–modulus mastercurves for the range of nanocomposites. These are illustrated in Fig. 7.

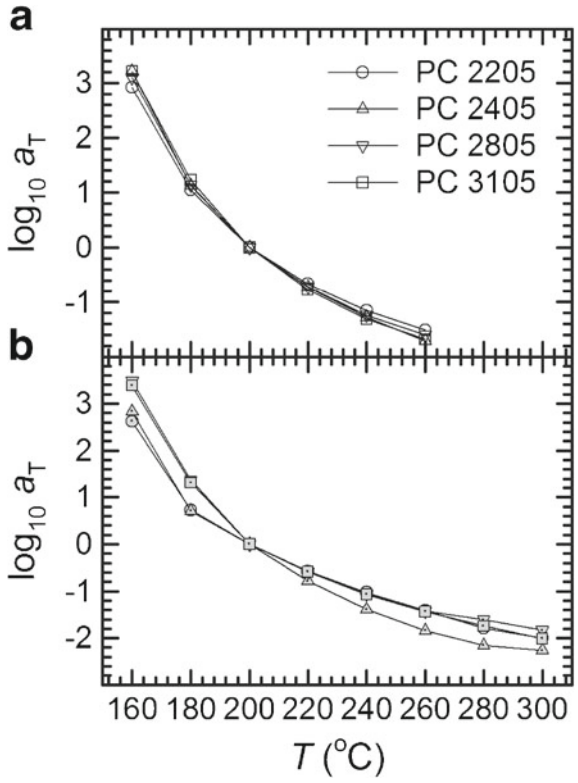

Fig. 5 Shift factors determined using an automated technique at $T_{ref} = 200$ °C. **a** Unfilled PC (*hollow symbols*) and (**b**) PC–MWCNT (3 wt%) (*dotted*, *grey symbols*). The *lines* are a guide to the eye

These mastercurves exhibit two important differences relative to those of the equivalent matrix polymers: (1) the presence of a second plateau instead of a zone of terminal flow and (2) a loss tangent that is less than unity throughout the extended frequency range. At low reduced frequencies, the second plateau has a modulus of $\sim 10^5$ Pa. This behaviour was first observed by Pötschke et al. (2002) for PC–MWCNT nanocomposites with more than 2 wt% filler content, sufficient to form a percolated network within the matrix system. Similar observations of network percolation for PC–MWCNT were reported in the works of Alig et al. (2008) and Skipa et al. (2009). The second plateau, approximately 1.5 orders of magnitude smaller than the rubbery plateau arising from the entanglement network, suggests the presence of an interconnected network of nanotubes and, hence, of rheological percolation.

The two-phase model of Song and Zheng (2010) was applied to the viscoelastic mastercurves of all matrix polymers and nanocomposites in order to clarify the nature of the changes in structure arising between the polymer and nanocomposite. This model is parameterised through a strain amplification factor parameter A_f, storage G'_{CNT} and loss G''_{CNT} modulus parameters representing the filler network, and an exponent α related to the frequency dependence of this filler network. Optimisation of the parameters

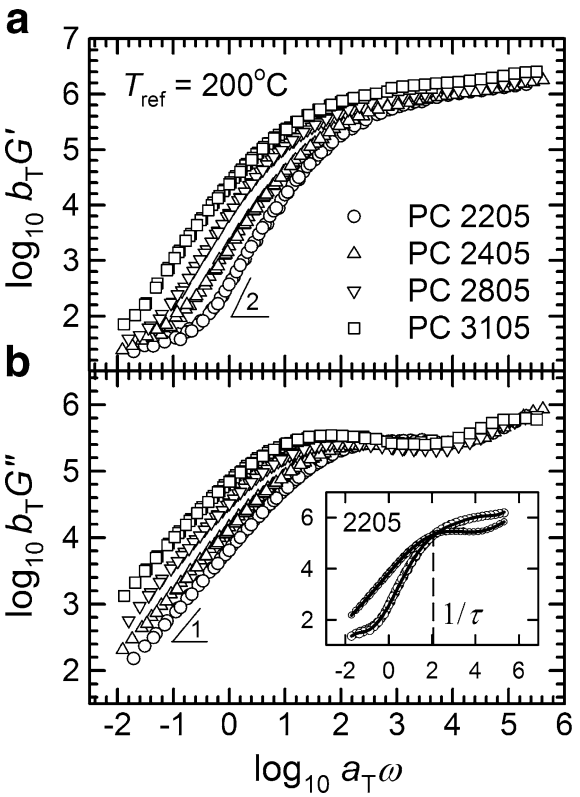

Fig. 6 Reduced frequency mastercurves of (**a**) storage modulus and (**b**) loss modulus of unfilled PC of varying molar mass ($M_w = 33{,}600$–$50{,}500$ g mol^{-1}) at a strain amplitude of 0.5 %. The *inset* shows the cross-over frequency for PC 2205 used to determine the characteristic relaxation time and a polynomial fit employed in the two-phase model (Song and Zheng 2010) (*thick solid line*)

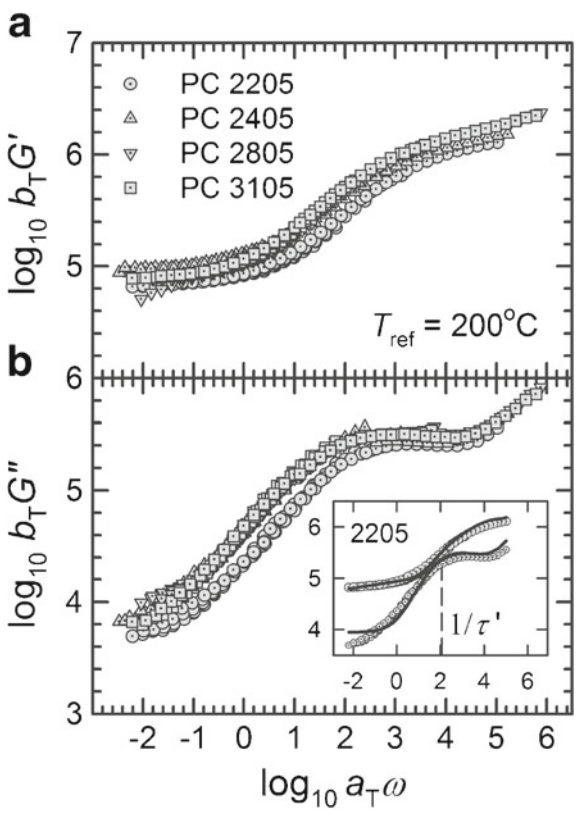

Fig. 7 Reduced frequency mastercurves of (**a**) storage modulus and (**b**) loss modulus of PC–MWCNT (3 wt%) with varying matrix molar mass ($M_w = 33{,}600$–$50{,}500$ g mol^{-1}) at a strain amplitude of 0.5 %. The *inset* shows the absence of a cross-over frequency for PC–MWCNT 2205 only, and the frequency at the peak in loss tangent used to determine the characteristic relaxation time, and the two-phase model (Song and Zheng 2010) fitted to the data (*thick solid line*)

was carried out following Song and Zheng's procedure, and fitted results are shown in the insets of Figs. 6 and 7 for filled and unfilled PC 2205. It was found that, in all PC grades, A_f did not exceed 1.35. The stiffness of the nanotube network $G'_{CNT} \sim 10^5$ Pa for all grades, and $G''_{CNT} \sim 10^4$ Pa. The frequency dependence of the network was negligible, with $\alpha \sim 10^{-2}$. Thus, the model is consistent with the view that the present systems do not exhibit pronounced strain amplification and that the nanotubes agglomerate into a mostly elastic network with stiffness $\sim 10^5$ Pa. The stiffness of this network is probably connected to nanotube bending modes (Rubinstein and Colby 2003).

The confinement of PC chains, if any, must therefore be localised to the surface of CNTs or CNT agglomerates. This is consistent with the T_g measurements of Table 2, and suggests that the earlier onset of deviation from the linearity observed during the amplitude sweeps in Fig. 1 for PC–MWCNT is caused by a destruction of the CNT network. Such a percolation network is known to exhibit gradual build-up with time in flocculation experiments (Richter et al. 2009), arising from diffusion-controlled agglomeration of MWCNTs (Zeiler et al. 2010).

Figure 8 illustrates the ratios of viscoelastic moduli of filled materials to those of pure materials as a function of reduced frequency. A ratio that deviates from unity is a signature that the nanotubes are influencing the viscoelastic

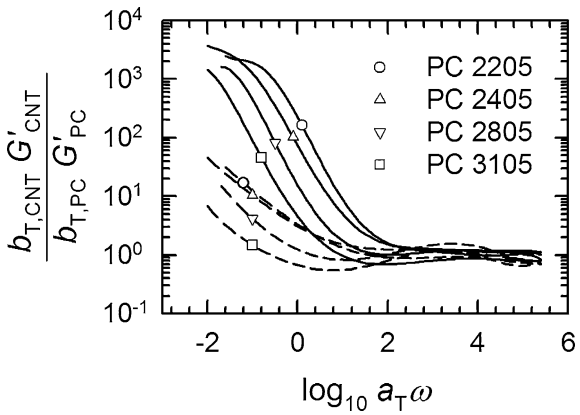

Fig. 8 Ratios of storage modulus (*solid line*) and loss modulus (*dashed line*) of filled PC–MWCNT (3 wt%) to unfilled PC of matching matrix molar mass ($M_w = 33{,}600$–$50{,}500$ g mol^{-1}) as a function of reduced frequency, determined at a strain amplitude of 0.5 %

response. The influence is greatest at the lowest reduced frequencies, where the pure polymer undergoes flow, but the filled system exhibits the second plateau. Here, the ratio of storage moduli exceeds 10^3, and the ratio of loss moduli exceeds 10. At higher reduced frequencies, the ratio is close to unity. A noteworthy feature is that the onset of the deviation from unity occurs at a lower reduced frequency (and hence longer timescale) with increasing molar polymer. Due to the substantial differences in size between polymer chains and CNTs, it is not unreasonable to assume that polymer mobility is the main driver for any rearrangement of the filler network and, hence, that the dominant relaxation mechanism observed is that of the polymer matrix.

Relaxation timescales

In the pure PC melts, a characteristic relaxation time τ was estimated from the inverse of the cross-over frequency for each grade, as shown in the inset of Fig. 6 for PC 2205. Linear regression was employed to identify the coefficient n of a power–law relationship of the form $\tau \propto M_w^n$, as shown in Fig. 9. n was identified as 5.66 ± 0.22 (where "±" refers to the standard deviation). This value is somewhat higher than the generally reported literature values of 3.4–3.75 for PC (Jordan and Richards 2000), and it is probable that the difference originates from the polydispersity of the commercial resins.

In the filled PC melts, it is not possible to obtain a characteristic relaxation time from the cross-over frequency since no cross-over occurs, as shown in the inset of Fig. 7. Nevertheless, the change in molar mass of the matrix polymer influences the mastercurves by shifting the frequency at which the reduction in the moduli takes place. Instead, a timescale τ' is determined corresponding to the inverse of the frequency at which the peak in tan δ occurs. The frequency is obtained for all grades on unshifted experimental data at 200 °C using a peak fitting algorithm. Linear regression was employed to identify the coefficient n of a power–law relationship of the form $\tau' \propto M_w^n$, and n was identified as 5.25 ± 0.62 (where ± refers to the standard deviation), as shown in Fig. 9.

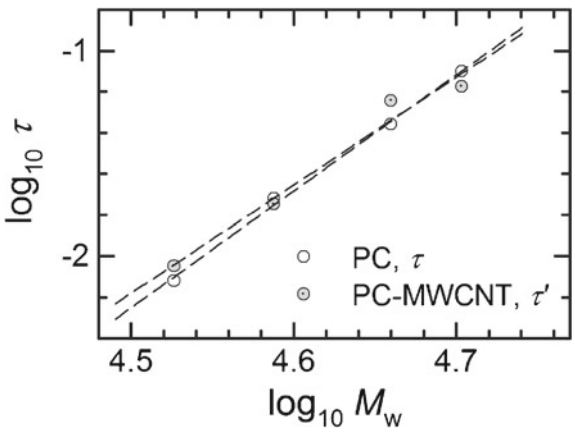

Fig. 9 Characteristic relaxation times obtained from the cross-over frequency in unfilled PC (*hollow symbols*) and from the peak in tan δ in the PC–MWCNT (3 wt%) (*dotted*, *grey symbols*), as a function of molar mass. The *dashed lines* represent linear regressions through the data sets

The two power–law coefficients are remarkably similar. In fact, by carrying out a paired Student's t test on the differences in relaxation times between filled and unfilled materials of equal matrix molar mass, we could not reject the hypothesis that the relaxation times are unaffected by the presence of nanotubes at a 90 % confidence level (two-tailed t test, $t = 0.48$, $n = 4$). This supports the view that the same relaxation mechanism applies to both pure PC melts and to nanocomposites. This implies that the molar mass of the matrix polymer affects the timescale of the relaxation process observed in the nanocomposites in the same way as it affects the pure polymers. The relaxation mechanism normally associated with polymer melts is reptation, although this generally scales with a lower power of molar mass than that recorded here.

Three types of interactions can be expected in a polymer nanocomposite: polymer–polymer interactions (dominated by the relaxation of the entanglement network), nanoparticle–nanoparticle interactions, and polymer–nanoparticle interactions (Pötschke et al. 2004). Only one type (polymer–polymer) is present in the unfilled polymers. The similarity in the scaling with molar mass of the relaxation processes observed is perhaps evidence of the key role played by polymer–polymer interactions in these filled systems. Although no conclusive evidence can be presented, it is reasonable to assume that nanotube–nanotube interactions are slow (given their size relative to polymer molecules) and limited in extent (by the small volume fraction), and that polymer–nanotube interactions are probably dominated by the faster relaxation of the polymer chains, and hence, that they also scale with molar mass in the same way as in the polymer–polymer interactions. Further evidence to support this is also available in the work of Zeiler et al. (2010), who observed an influence of molar mass of the matrix on the dynamics of network formation in nanocomposites.

Although no estimate of relaxation time of a nanotube–nanotube network can be made, the fact that these materials can be melt compounded and extruded is clear evidence that they will flow if sufficient shear stress is applied. Another interpretation of this is that the applied stress reduces the relaxation time of the nanotube network to the timescale of the experiment (Costa et al. 2008; Richter et al. 2009).

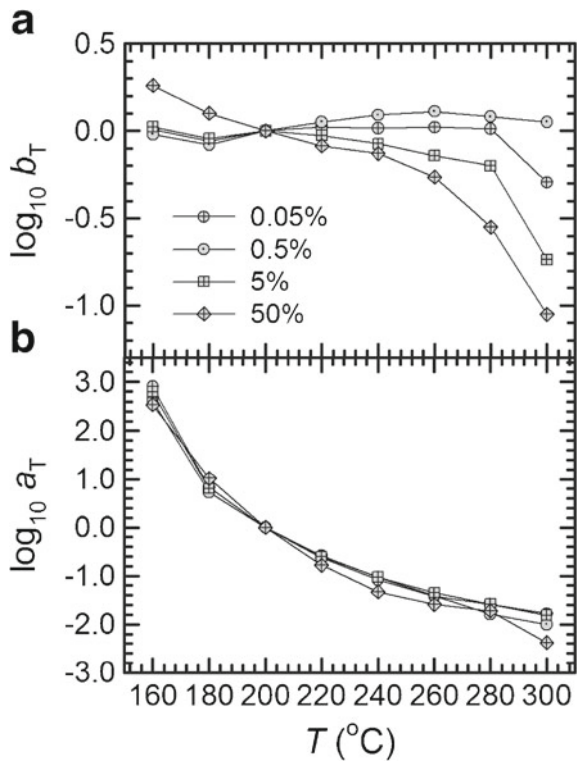

Fig. 10 **a** Vertical shift factors and (**b**) horizontal shift factors obtained from isothermal frequency sweeps at strain amplitudes of 0.05, 0.5, 5 and 50 % at T_{ref} = 200 °C. The *lines* are a guide to the eye

Large amplitude viscoelastic response

In order to probe the material response in the non-linear regime, mastercurves were constructed from isothermal frequency sweeps conducted at strain amplitudes of 0.05, 5, and 50 %, by appropriate vertical and horizontal shifting. Vertical shifting was performed manually using VGP plots, and the vertical shift factors are illustrated in Fig. 10a as a function of strain amplitude. Horizontal shift factors were subsequently determined for each strain amplitude using the automated technique,[2] and these are shown in Fig. 10b.

The effect of increasing the strain amplitude is much greater on the vertical shift factors than on the horizontal shift factors. The small effect on the horizontal shift factors suggests that strain amplitude is not significantly affecting the relaxation mechanisms and their temperature dependence. This is consistent with the view that polymer matrix relaxation is the dominant mechanism and with the small amplitude dependence observed on the moduli from the amplitude sweeps on pure PC in Fig. 1.

[2]For the highest test temperatures only ($T \geq 280$ °C), the horizontal shift factors could not be obtained automatically due to the reduced dependence of modulus on the frequency. Instead, they were determined manually from a visual assessment.

The vertical shift factors are most affected by amplitude at the highest test temperature, where shifting to a lower reference temperature requires a reduction of modulus. This can be understood by considering a nanotube network that is affected by two processes: strain amplitude (setting the degree of network disruption) and temperature (affecting the kinetics of network formation). Thus, the higher the test temperatures (where the network will approach an equilibrium state more quickly), the stiffer the equilibrium state of the nanotube network for a given strain amplitude. At lower test temperatures, the state of the nanotube network will be further from equilibrium and, hence, more history-dependent.

Mastercurves constructed from shifted isothermal frequency sweeps performed across the range of strain amplitudes on PC 2205 shifted to a reference temperature of 200 °C, and these are shown in Fig. 11. There is little difference between the 0.05 and 0.5 % strain amplitudes other than the increased noise at 0.05 % because of smaller torque and angular velocity signals. When the amplitude increases to 5 %, it is still possible to construct a mastercurve with good overlap between the test temperatures. There is evidence of shear thinning, with moduli reducing by almost one order of magnitude across the extended reduced frequency. At 50 % strain amplitude, the procedure of constructing

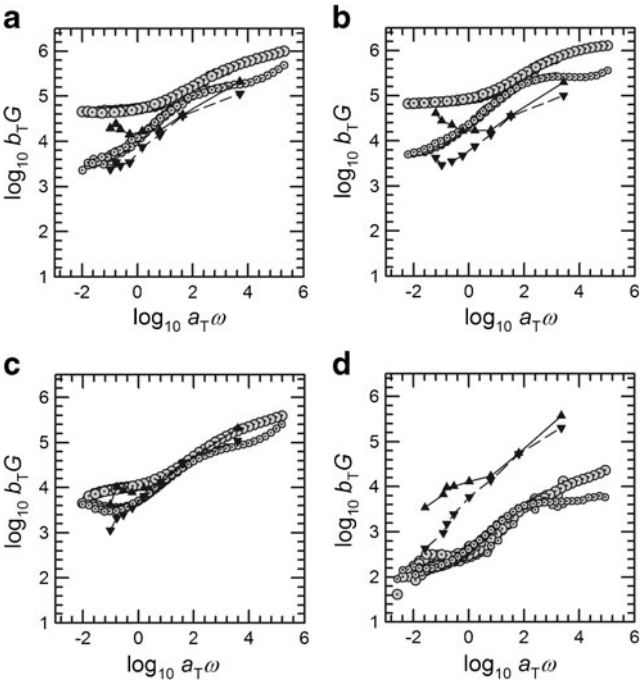

Fig. 11 Mastercurves for filled PC–MWCNT 2205 (3 wt%) (G', *large dotted grey circles*; G'', *small dotted grey circles*) for strain amplitudes of (**a**) 0.05, (**b**) 0.5, (**c**) 5 and (**d**) 50 %, at $T_{ref} = 200$ °C. Corresponding measurements obtained from amplitude sweeps (G', *up-pointing triangles*; G'', *down-pointing triangles*) measured at 2π rad s^{-1}. The *solid* and *dashed lines* are a guide to the eye

the mastercurve is more challenging as there is less overlap between temperatures. The moduli are as much as two orders of magnitude smaller at 50 % strain amplitude than at 0.5 %.

The reduction in moduli across the reduced frequency range indicates that the strain amplitude is affecting both the nanotube network and the entanglement network. For a given strain amplitude, however, the effect is larger at the low reduced frequency end of the spectrum, where the nanotube network dominates, than at the high reduced frequency end where the entanglement network dominates.

Roles of strain and temperature history

The strain and temperature history experienced by a nanocomposite plays an important role in defining the extent to which the nanotube network is developed and, hence, the extent to which it contributes to the response. This build-up is readily observable through flocculation experiments such as those of Richter and co-workers (2009). The effect is also observable in the present experiments by comparing the responses measured at identical reduced frequencies and strain amplitudes obtained from frequency sweeps and from amplitude sweeps.

Moduli obtained during the amplitude sweeps at a range of temperatures shown in Fig. 1 measured at strain amplitudes closest to 0.05, 0.5, 5, and 50 %[3] at fixed frequency 2π rad s^{-1} were first shifted vertically according to the shift factors shown in Fig. 10a. Then, TTS was employed to shift the frequency to a reference temperature of 200 °C to allow a direct comparison with the large amplitude frequency sweeps. These measurements are also shown in Fig. 11.

Differences in strain and temperature history are responsible for the differences in moduli between the mastercurves based on frequency sweeps and those extracted from amplitude sweeps. It is worth restating that the amplitude sweeps were performed on a single specimen across a reducing temperature range from 300 to 160 °C, with each temperature experiencing increasing strain levels through to 100 % prior to cooling and acclimatising at the next temperature. This means that the history of every amplitude sweep measurement except the first (at 300 °C) is of a nanotube structure that has been disrupted by the brief application of 100 % strain at the previous temperature and that has reformed to a certain degree during the allowed acclimatisation time of 5 min. Frequency sweeps were instead performed across the same reducing temperature range from 300 to 160 °C, but each specimen experienced a fixed strain amplitude (of 0.05, 0.5, 5 and 50 %) at all temperatures.

[3]The actual strain amplitudes were 0.043 ± 0.001, 0.49 ±0.002, 5.4 ± 0.1and 57 ± 11 %.

By comparing the mastercurves obtained from the two methods, it is apparent that only the moduli measured at 5 % strain are almost identical, whereas the moduli obtained at 0.05, 0.5 and 50 % strain are not so. The implication of the nearly identical moduli at 5 % strain is that the structure of the nanotube network must be comparable. In the case of the frequency sweep, it has experienced a 5 % strain amplitude throughout the frequency range at each temperature, followed by a recovery period whilst changing temperature. In the case of the amplitude sweep, it has experienced up to 100 % strain amplitude at the previous measurement temperature, followed by a recovery period whilst changing temperature, and a rising amplitude through to 5 %. Thus, we can speculate that the level of network disruption and build-up obtained following a constant 5 % strain amplitude is similar to that obtained following a brief 100 % disruption, a recovery period of 5.5 min in which the temperature is reducing and settling, and a rising amplitude through to 5 % strain.

The same moduli are not obtained following the two histories through to the other strains. For the smaller strain amplitudes 0.05 and 0.5 %, the disruption caused during the amplitude sweeps at 100 % strain at the previous test temperature results in a lower modulus. For the larger strain amplitude 50 %, there is greater disruption to the network during the constant 50 % amplitude frequency sweep than during the rising amplitude sweep.

This comparison between amplitude sweep and frequency sweep measurements serves as a reminder of the particular challenges of characterising a material whose properties are very sensitive to strain and temperature history, and highlights the need for detailed methodologies of characterisation to enable reproducible results and thorough understanding to be achieved.

Conclusions

This paper has investigated the linear and non-linear viscoelastic response of four grades of PC melt compounded with 3 wt% MWCNTs and of the matching matrix polymers.

Isothermal amplitude sweeps performed over a wide temperature range indicated that the nanocomposites deviate from linear viscoelasticity at much smaller strains relative to the pure polymers. Although this has been attributed to strain amplification, where the matrix polymer experiences a higher local strain than the macroscopic strain due to the presence of the stiff nanotubes network, evidence suggests that disruption of the nanotube network at increasing strain amplitudes is responsible. This is consistent with a lack of change of mobility interpreted from T_g measurements. Filled materials also exhibit a strain overshoot in loss modulus not seen in the pure polymer.

Isothermal frequency sweeps were carried out on both MWCNT-filled and pure materials. The effect of temperature on modulus was accounted for by employing a density correction to the modulus in pure materials and a shift obtained from van Gurp-Palmen plots in the filled materials. Mastercurves were then constructed by employing an automated shifting procedure to identify horizontal shift factors for time–temperature superposition. The horizontal shift factors were found to be relatively independent of both matrix polymer and the presence of nanotubes, suggesting that relaxation processes have the same temperature dependence in filled and pure materials. The filled mastercurves exhibit two distinct differences from the pure polymer: a second plateau at low reduced frequency with a modulus of $\sim 10^5$ Pa, associated with a percolated nanotube network, and a loss tangent less than unity across the extended frequency range. Evidence of the filler network's contribution to the modulus was observed through application of the Song and Zheng's two-phase model. Relaxation timescales of both unfilled and filled materials were approximated from the inverse of the cross-over frequency and the frequency at the peak in the loss tangent, respectively. All these timescales scale with molar mass through a power–law with very similar coefficients, a further evidence that the dominant relaxation mechanism in the nanocomposites is associated with the polymer network itself.

Isothermal frequency sweeps were carried out at varying strain amplitudes from 0.05 to 50 % and horizontal and vertical shift factors obtained to produce mastercurves. There was a considerable effect of strain amplitude on the vertical shifting, arising from the different levels of disruption to the nanotube network from the strain amplitudes. The effect of strain amplitude on horizontal shifting was small, even at 50 % strain. A comparison of moduli obtained at the same reduced frequency and amplitude from two different experiments was carried out to illustrate how strain and temperature history can affect the magnitude of the viscoelastic response of nanocomposite materials.

Acknowledgments The authors gratefully acknowledge the contribution of Dr. Andy C.Y. Lew from Nanocyl S.A. for the supply and compounding of the nanocomposites; of Dr. Jaouad El Harfi from the University of Nottingham for the assistance with the Soxhlet extraction process; and of Dr. Jaouad El Harfi and Dr. Natasha Birkin from the University of Nottingham for the assistance with the GPC measurements.

Appendix: Automated technique for the identification of horizontal shift factors

The technique employed in this work to identify horizontal shift factors for TTS is broadly based on that suggested by Gergesova et al. (2010). It is aimed at removing the ambiguity normally present in manual shifting of viscoelastic experimental data. The method is based on an optimisation technique seeking to identify the shift factor that minimises the area enclosed by overlapping moduli between viscoelastic data measured at adjacent temperatures.

The first step in the procedure is the definition of a reference temperature T_{ref}. A MATLAB optimisation subroutine is then used to identify the coefficients of a set of polynomials $f_{T_i}^{b_T G'}(\log \omega)$ and $f_{T_i}^{b_T G''}(\log \omega)$ that best fit each set of measured values of reduced log G' and log G'' as a function of log frequency, for each measured temperature. In the present data, a third-order polynomial was found to be satisfactory. Figure 12 illustrates the polynomial fitting of experimental data of viscoelastic moduli for pure PC 2205 measured at $T = 160 - 260$ °C. The polynomials are used in the subsequent shift factor optimisation instead of the measured experimental data in order to minimise the consequences of experimental scatter.

For each pair of temperatures T_i and T_{i+1}, an overlap region is identified for both storage and loss moduli. Each region is enclosed by the two polynomials obtained from the data at the two temperatures of interest on the left and right boundaries. The lower boundary is defined by the value of the polynomial functions

$$f_{T_i}^{b_T G'}(\min(\log \omega)) \quad \text{and} \quad f_{T_i}^{b_T G''}(\min(\log \omega)) \tag{4}$$

where min(log ω) is the log of the smallest frequency recorded experimentally for T_i. The upper boundary is defined similarly by the values of the polynomial functions

$$f_{T_{i+1}}^{b_T G'}(\max(\log \omega)) \quad \text{and} \quad f_{T_{i+1}}^{b_T G''}(\max(\log \omega)) \tag{5}$$

where max(log ω) is the log of the highest frequency recorded experimentally at T_{i+1}.

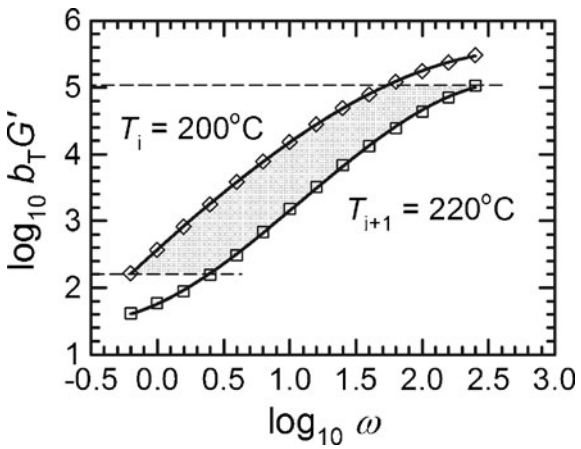

Fig. 12 Illustration of the construction of the area (*shaded*) minimised to determine the optimum shift factor. The *solid lines* are polynomial functions. The *dashed lines* represent the upper and lower boundaries of the overlapping area

An optimisation routine is scripted in MATLAB to identify the value of the shift factor, a_T such that when the shifting is applied to the polynomials, giving $f_{T_i+1}^{b_\top G}(\log a_T \omega)$ and $f_{T_i+1}^{b_\top G}(\log a_T \omega)$, the sum of the magnitudes of the overlap regions obtained simultaneously from storage and loss moduli data is a minimum.

The construction of a single bound area is illustrated on real experimental data for pure PC 2205 in Fig. 12, with $T_i = 200$ °C and $T_{i+1} = 220$ °C. Each area was computed numerically using the trapezium rule. A shift factor was obtained between each pair of neighbouring temperatures, and the values reported are relative to the reference temperature.

References

Abdel-Goad M, Pötschke P (2005) Rheological characterization of melt processed polycarbonate-multiwalled carbon nanotube composites. J Non-Newton Fluid Mech 128(1):2–6. doi:10.1016/j.jnnfm.2005.01.008

Alig I, Skipa T, Lellinger D, Pötschke P (2008) Destruction and formation of a carbon nanotube network in polymer melts: rheology and conductivity spectroscopy. Polymer 49(16):3524–3532. doi:10.1016/j.polymer.2008.05.037

Alig I, Pötschke P, Lellinger D, Skipa T, Pegel S, Kasaliwal GR, Villmow T (2012) Establishment, morphology and properties of carbon nanotube networks in polymer melts. Polymer 53(1):4–28. doi:10.1016/j.polymer.2011.10.063

Bayer Material Science AG (2009) Makrolon 2205 and 2207 polycarbonate resins. Bayer Material Science AG, Edition 2009-05-11. Bayer Material Science AG, Leverkusen

Cadek M, Coleman JN, Barron V, Hedicke K, Blau WJ (2002) Morphological and mechanical properties of carbon-nanotube-reinforced semicrystalline and amorphous polymer composites. Appl Phys Lett 81(27):5123–5125. doi:10.1063/1.1533118

Castillo FY, Socher R, Krause B, Headrick R, Grady BP, Prada-Silvy R, Pötschke P (2011) Electrical, mechanical, and glass transition behavior of polycarbonate-based nanocomposites with different multi-walled carbon nanotubes. Polymer 52(17):3835–3845. doi:10.1016/j.polymer.2011.06.018

Costa F, Saphiannikova M, Wagenknecht U, Heinrich G (2008) Layered double hydroxide based polymer nanocomposites. Adv Polym Sci 210:101–168. doi:10.1007/12_2007_123

Curran SA, Talla J, Dias S, Zhang D, Carroll D, Birx D (2009) Electrical transport measurements of highly conductive carbon nanotube/poly(bisphenol A carbonate) composite. J Appl Phys 105(7):073711–073715. doi:10.1063/1.3073938

Dealy J, Plazek D (2009) Time-temperature superposition—a users guide. Rheol Bull 78(2):16–32

Dijkstra D, Cirstea M, Nakamura N (2010) The orientational behavior of multiwall carbon nanotubes in polycarbonate in simple shear flow. Rheol Acta 49(7):769–780. doi:10.1007/s00397-010-0457-6

Du F, Scogna RC, Zhou W, Brand S, Fischer JE, Winey KI (2004) Nanotube networks in polymer nanocomposites: rheology and electrical conductivity. Macromolecules 37(24):9048–9055. doi:10.1021/ma049164g

Eitan A, Fisher FT, Andrews R, Brinson LC, Schadler LS (2006) Reinforcement mechanisms in MWCNT-filled polycarbonate. Compos Sci Technol 66(9):1162–1173. doi:10.1016/j.compscitech.2005.10.004

Fisher FT, Bradshaw RD, Brinson LC (2002) Effects of nanotube waviness on the modulus of nanotube-reinforced polymers. Appl Phys Lett 80(24):4647–4649. doi:10.1063/1.1487900

Fornes TD, Baur JW, Sabba Y, Thomas EL (2006) Morphology and properties of melt-spun polycarbonate fibers containing single- and multi-wall carbon nanotubes. Polymer 47(5):1704–1714. doi:10.1016/j.polymer.2006.01.003

Gergesova M, Zupančič B, Saprunov I, Emri I (2010) The closed form t-T-P shifting (CFS) algorithm. J Rheol 55(1):1–16. doi:10.1122/1.3503529

Handge U, Pötschke P (2007) Deformation and orientation during shear and elongation of a polycarbonate/carbon nanotubes composite in the melt. Rheol Acta 46(6):889–898. doi:10.1007/s00397-007-0179-6

Handge U, Zeiler R, Dijkstra D, Meyer H, Altstädt V (2011) On the determination of elastic properties of composites of polycarbonate and multi-wall carbon nanotubes in the melt. Rheol Acta 50(5):503–518. doi:10.1007/s00397-011-0558-x

Hyun K, Wilhelm M, Klein CO, Cho KS, Nam JG, Ahn KH, Lee SJ, Ewoldt RH, McKinley GH (2011) A review of nonlinear oscillatory shear tests: analysis and application of large amplitude oscillatory shear LAOS. Prog Polym Sci 36(12):1697–1753. doi:10.1016/j.progpolymsci.2011.02.002

Jordan TC, Richards WD (2000) Polycarbonate melt rheology. In: Legrand DG, Bendler JT (eds) Handbook of polycarbonate science and technology. Marcel Dekker, New York, pp 179–224

Lew CY, Xia H, McNally T, Fei G, Vargas J, Millar B, Douglas P, Claes M, Luizi F (2009) A unified strategy to incorporating nanotube in twinscrew extrusion processing. In: Polymer processing society europe/africa regional meeting. Larcana, Cyprus

Lew CY, Dewaghe C, Claes M (2011) Injection moulding of polymer–carbon nanotubes. In: McNally T, Pötschke P (eds) Polymer-carbon nanotube composites: preparation, properties and applications. Woolhead, Cambridge, pp 155–192

Pötschke P, Fornes TD, Paul DR (2002) Rheological behavior of multiwalled carbon nanotube/polycarbonate composites. Polymer 43(11):3247–3255. doi:10.1016/S0032-3861(02)00151-9

Pötschke P, Abdel-Goad M, Alig I, Dudkin S, Lellinger D (2004) Rheological and dielectrical characterization of melt mixed polycarbonate-multiwalled carbon nanotube composites. Polymer 45(26):8863–8870. doi:10.1016/j.polymer.2004.10.040

Pötschke P, Brünig H, Janke A, Fischer D, Jehnichen D (2005) Orientation of multiwalled carbon nanotubes in composites with polycarbonate by melt spinning. Polymer 46(23):10355–10363. doi:10.1016/j.polymer.2005.07.106

Reichert P, Hoffmann B, Bock T, Thomann R, Mülhaupt R, Friedrich C (2001) Morphological stability of poly(propylene) nanocomposites. Macromol Rapid Commun 22(7):519–523. doi:10.1002/1521-3927(20010401)22:7<519::aid-marc519>3.0.co;2-w

Richter S, Saphiannikova M, Jehnichen D, Bierdel M, Heinrich G (2009) Experimental and theoretical studies of agglomeration effects in multi-walled carbon nanotube-polycarbonate melts. Express Polym Lett 3(12):753–768. doi:10.3144/expresspolymlett.2009.94

Rubinstein M, Colby RH (2003) Polymer physics. Oxford, Oxford University Press

Saphiannikova M, Skipa T, Lellinger D, Alig I, Heinrich G (2012) Superposition approach for description of electrical conductivity in sheared MWNT/polycarbonate melts. Express Polym Lett 6(6):438–453. doi:10.3144/expresspolymlett.2012.47

Satapathy BK, Weidisch R, Pötschke P, Janke A (2007) Tough-to-brittle transition in multiwalled carbon nanotube MWNT/poly-

carbonate nanocomposites. Compos Sci Technol 67(5):867–879. doi:10.1016/j.compscitech.2006.01.036

Shaffer MSP, Windle AH (1999) Fabrication and characterization of carbon nanotube/poly(vinyl alcohol) composites. Adv Mater 11(11):937–941. doi:10.1002/sici1521-4095(199908)11:11<937::aid-adma937>3.0.co;2-9

Skipa T, Lellinger D, Böhm W, Saphiannikova M, Alig I (2009) Influence of shear deformation on carbon nanotube networks in polycarbonate melts: interplay between build-up and destruction of agglomerates. Polymer 51(1):201–210. doi:10.1016/j.polymer.2009.11.047

Solomon MJ, Almusallam AS, Seefeldt KF, Somwangthanaroj A, Varadan P (2001) Rheology of polypropylene/clay hybrid materials. Macromolecules 34(6):1864–1872

Song Y, Zheng Q (2010) Linear viscoelasticity of polymer melts filled with nano-sized fillers. Polymer 51(14):3262–3268. doi:10.1016/j.polymer.2010.05.018

Spitalsky Z, Tasis D, Papagelis K, Galiotis C (2010) Carbon nanotube-polymer composites: chemistry, processing, mechanical and electrical properties. Prog Polym Sci 35(3):357–401. doi:10.1016/j.progpolymsci.2009.09.003

Stöckelhuber KW, Svistkov AS, Pelevin AG, Heinrich G (2011) Impact of filler surface modification on large scale mechanics of styrene butadiene/silica rubber composites. Macromolecules 44(11):4366–4381. doi:10.1021/ ma1026077

Sung YT, Kum CK, Lee HS, Byon NS, Yoon HG, Kim WN (2005) Dynamic mechanical and morphological properties of polycarbonate/multi-walled carbon nanotube composites. Polymer 46(15):5656–5661. doi:10.1016/j.polymer.2005.04.075

Sung YT, Han MS, Song KH, Jung JW, Lee HS, Kum CK, Joo J, Kim WN (2006) Rheological and electrical properties of polycarbonate/multi-walled carbon nanotube composites. Polymer 47(12):4434–4439. doi:10.1016/j.polymer.2006.04.008

van Gurp M, Palmen J (1998) Time-temperature superposition for polymeric blends. Rheol Bull 67(1):1–5

Vilgis TA (2005) Time scales in the reinforcement of elastomers. Polymer 46(12):4223–4229. doi:10.1016/j.polymer.2005.02.060

Wan T, Clifford MJ, Gao F, Bailey AS, Gregory DH, Somsunan R (2005) Strain amplitude response and the microstructure of PA/clay nanocomposites. Polymer 46(17):6429–6436. doi:10.1016/j.polymer.2005.04.105

Wu D, Wu L, Zhang M (2007) Rheology of multi-walled carbon nanotube/poly(butylene terephthalate) composites. J Polym Sci B Polym Phys 45(16):2239–2251. doi:10.1002/polb.21233

Yamamoto G, Suk JW, An J, Piner RD, Hashida T, Takagi T, Ruoff RS (2010) The influence of nanoscale defects on the fracture of multi-walled carbon nanotubes under tensile loading. Diamond Relat Mater 19(7–9):748–751. doi:10.1016/j.diamond.2010.01.045

Zeiler R, Handge UA, Dijkstra DJ, Meyer H, Altstädt V (2010) Influence of molar mass and temperature on the dynamics of network formation in polycarbonate/carbon nanotubes composites in oscillatory shear flows. Polymer 52(2):430–442. doi:10.1016/j.polymer.2010.11.037

Zoller P (1982) A study of the pressure-volume-temperature relationships of four related amorphous polymers: polycarbonate, polyarylate, phenoxy, and polysulfone. J Polym Sci Polym Phys Ed 20(8):1453–1464. doi:10.1002/pol.1982.180200811